Pathogenesis, biophysical stability and phenotypic variance of SAT2 foot-and-mouth disease virus

Tovhowani D. Ramulongo[a,b,1], Francois F. Maree[a,b,1], Katherine Scott[a], Pamela Opperman[a,c], Paidamwoyo Mutowembwa[d], Jacques Theron[c]

[a]Transboundary Animal Diseases, Vaccine and Diagnostic Development Programme, Onderstepoort Veterinary Research Institute, Agricultural Research Council, Onderstepoort, Pretoria, 0110, South Africa
[b]Department of Biochemistry, Genetics and Microbiology, Faculty of Natural and Agricultural Sciences, University of Pretoria, Pretoria, 0002, South Africa
[c]Department Animal Production Studies, Faculty of Veterinary Sciences, University of Pretoria, Pretoria, 0110, South Africa
[d]Transboundary Animal Diseases, Vaccine Production Programme, Onderstepoort Veterinary Research Institute, Agricultural Research Council, Onderstepoort, Pretoria, 0110, South Africa

∗Corresponding author at: Private Bag X05, Onderstepoort, 0110, South Africa.
E-mail address: mareef@arc.agric.za (F.F. Maree).

[1] Joint first authors

Highlights

•FMD clinical signs range from mild to severe or subclinical.
•Pathogenesis of SAT2 viruses did not correlate with cell killing or viral fitness.
•SAT2 viruses have a wide range of lability at low pH or high temperatures.
•No correlation was found between biophysical stability and pathogenesis.
•Effective control of SAT2 viruses needs to consider variance in biological phenotypes.

Abstract

Foot-and-mouth disease (FMD) is a highly contagious vesicular disease of cloven-hoofed animals, which severely decreases livestock productivity. FMD virus (FMDV), the causative agent, initiates infection by interaction with integrin cellular receptors on pharyngeal epithelium cells, causing clinical signs one to four days after transmission to a susceptible host. However, some Southern African Territories (SAT) viruses have been reported to cause mild or subclinical infections that may go undiagnosed in field conditions and are likely to be more common than previously expected. The studies presented here demonstrate that not all SAT2 viruses are equally virulent in cattle. The two SAT2 viruses, ZIM/5/83 and ZIM/7/83, were both highly attenuated in cattle, as evidenced by the mild clinical signs observed after needle challenge, while two incongruent SAT2 viruses showed significantly different clinical signs in challenged cattle. We then explored the ability of the SAT2 viruses to infect different cell types with defined receptors that are utilised by FMDV and found differences in their ability to lyse cells in culture and to compete in a controlled cell culture environment. The population sequence variation between ZIM/5/83 and ZIM/7/83 revealed multiple sites of single nucleotide variants of low frequency between the predominant virus populations, as could be expected from the genome of an RNA virus. An assessment of the biophysical stability of SAT2 virions during acidification indicated that the SAT2 virus EGY/09/12 was

more resilient to acidification than the ZIM/5/83 and ZIM/7/83 viruses; however, whether this difference relates to differences in virulence *in vivo* is unclear. This study is a consolidated view of the key findings of SAT2 viruses studied over a 14-year period involving many different experiments.

Keywords: Foot-and-mouth disease virus; Southern African Territories type 2; Pathogenesis; Genetic diversity; pH stability; Replicative fitness

Importance

Foot-and-mouth disease SAT2 virus causes a range of clinical signs that may vary from mild to severe or subclinical with no obvious lesions or fever in its host. However, due to within host variation, some animals may become infected and excrete the virus despite not developing clinical signs of the disease. This is a major concern for control strategies. The variance in pathogenesis of SAT2 viruses did not correlate with cell lysis ability in cultured cells or viral fitness during co-infection of cultured cells. The biophysical stability of SAT2 viruses revealed that SAT2 viruses have a wide range of lability at low pH or high temperatures with no direct correlation with pathogenesis. The effective control of SAT2 viruses needs to consider variance in biological phenotypes attributed to survival and increased spread.

1. Introduction

Foot-and-mouth disease (FMD) is a highly contagious vesicular disease of cloven-hoofed animals, causing significant distress and suffering to animals. Although mortality is usually low (<5%), morbidity can reach 100 % and cause severe losses in livestock production (Knight-Jones and Rushton, 2013). For that reason, FMD is classified by the Office International des Epizooties (OIE) as one of the most important infectious diseases of animals (OIE Manual, 2018).

FMD virus (FMDV) is a positive-sense, single-strand RNA virus belonging to the genus *Aphthovirus* in the family *Picornaviridae*. The viral genome is comprised of >8000 nucleotides and is enclosed by an icosahedral protein capsid comprised of 60 copies of four structural proteins with VP1 (1D), VP2 (1B), and VP3 (1C) surface exposed and VP4 (1A) buried within the capsid Acharya et al., 1989; Logan et al., 1993). The outer capsid proteins are directly involved in antigenicity with more than 40 % of the residues exposed on the virion surface (Reeve et al., 2010). Amino acid substitutions in any of the surface-exposed structural loops result in antigenic variation of the virus (Feigelstock et al., 1992; Maree et al., 2011). FMDV initiates cell entry in cultured cells or in the susceptible host through the arginine-glycine-aspartic acid (RGD) motif located in a flexible βG-βH loop of VP1, which recognises any of the four RGD-dependent integrin receptors, $\alpha_v\beta_1$, $\alpha_v\beta_3$, $\alpha_v\beta_6$ and $\alpha_v\beta_8$ (Berinstein et al., 1995; Jackson et al., 2000, 2002; Neff et al., 2000), therafter capsid dissociation through acidification within endosomes occurs. Cell culture-adapted FMDV strains acquire positively charged residues on the surface-exposed VP1 capsid protein, resulting in cell infection through alternative cellular glycosaminoglycan (GAG) receptors, like heparan sulfate proteoglycans (HSPG) (Jackson et al., 1996; Sa-Carvalho et al., 1997). FMDV cell entry may also be mediated by integrin- and heparan sulfate (HS)-independent

pathways like the cell membrane phosphatidylserine receptor containing protein 6 of the Jumonji-C domain (JMJD6) (Lawrence et al., 2016).

Whilst the VP1 protein is significant for virus attachment and entry, protective immunity and serotype specificity (Acharya et al., 1989), the VP2 and VP3 proteins play a critical role in virion structural stability and maturation (Curry et al., 1997; Kotecha et al., 2015). Although FMDV needs to be acid labile to permit efficient uncoating, its capsid must also be robust enough to shield the genome from the extracellular environment (Ellard et al., 1999).

FMD is endemic in large parts of Africa. The disease is unlikely to be eradicated from southern and eastern Africa due to the presence of large numbers of the free-living maintenance host, the African buffalo (*Syncerus caffer*), which provide a potential source of infection for domestic livestock and wildlife (Dawe et al., 1994; Thomson et al., 2003; Casey-Bryars et al., 2018). The infected buffalo pose a constant threat to susceptible livestock, as evidenced by several outbreaks that have occurred in southern Africa since 2000 (caused by SAT1 and SAT2), including South Africa, Namibia, Botswana, Zimbabwe, Mozambique, Zambia and Malawi (Records of the OIE). FMD epidemiology in North Africa is complicated by the co-circulation of endemic FMD viruses, as well as sporadic incursions of exotic viruses from the Middle East and sub-Saharan Africa (Ahmed et al., 2012). During 2012, there was a dramatic increase in SAT2 outbreaks in Egypt with cattle, water buffalo and small ruminants affected with severe clinical signs, especially in young animals (Ahmed et al., 2012). Since its emergence in North Africa, this SAT2 virus, belonging to topotype VII, has spread to Libya and Palestine (2012), Mauritania (2014) and Oman (2015).

Five of the seven FMDV serotypes, excluding Asia-1 and type C, have occurred on the African continent within the last decade, with the SAT serotypes generally confined to sub-Saharan Africa (Rweyemamu et al., 2008). The SAT types display large genetic and antigenic variability, as well as regional differences in the distribution and prevalence of serotypes (Bronsvoort et al., 2004; Maree et al., 2011; Casey-Bryars et al., 2018). Geographically, SAT2 is the most widely distributed serotype throughout sub-Saharan Africa and is also the most frequently associated with outbreaks in southern Africa (Vosloo et al., 2002; Rweyemamu et al., 2008). Despite having controlled FMD successfully through vaccination for many years in countries like Botswana and South Africa, the re-emergence of FMD in southern Africa has increased since 2009. Of particular concern is that in 2011 both countries experienced outbreaks caused by SAT viruses within recognized FMD-free areas. Control is further complicated by the fact that some SAT viruses have been reported to cause mild or subclinical infections that may go undiagnosed under field conditions and are likely to be more common than previously expected (Jori et al., 2009).

Here, we investigated the pathogenesis, relative infectivity, genetic variability, virus fitness and biophysical stability of SAT2 viruses. To this end, two related (SAT2/ZIM/5/83 and SAT2/ZIM/7/83) and two incongruent (SAT2/ZIM/14/90 and chimeric SAT2/EGY/9/12) SAT2 viruses were used. The SAT2/ZIM/5/83 virus has a low passage history and caused an outbreak in cattle in the western part of Zimbabwe in 1983, whereas SAT2/ZIM/7/83 has been passaged multiple times, and is the vaccine strain derived from SAT2/ZIM/5/83. In contrast, SAT2/ZIM/14/90 and SAT2/EGY/9/12 are virulent viruses and belong to the different geographically dispersed topotypes II and VII, respectively. The results obtained indicated that SAT2 viruses have a wide range of lability at low pH or high temperatures, replication dynamics and fitness in cultured cells related to the number of passages, and cause

mild to severe clinical or subclinical signs in cattle. This study is a consolidated view of the key findings of SAT2 viruses studied over a 14-year period.

2. Materials and methods

2.1. Cell lines and viruses

Baby hamster kidney-21 (BHK-21, clone 13, ATCC CCL-10) cells were maintained and propagated in Eagle's basal medium (BME; Life Technologies), as described previously (Rieder et al., 1993). Instituto Biologico renal suino (IB-RS-2 or RS) cells were maintained in RPMI medium (Sigma-Aldrich) or Ham's F-12 medium (Invitrogen). Foetal goat tongue cells (ZZ-R 127; Brehm et al., 2009) were maintained in DMEM Ham's F-12 (Sigma-Adrich). Chinese hamster ovary (CHO) cells strains K1 (ATCC CCL-61), 677 (ATCC CRL-2244) and 745 (ATCC CRL-2242) were propagated in Ham's F-12 Nutrient Mixture (Sigma-Adrich), whilst the lec2 cells (ATCC CRL-1736) were maintained in Minimum Essential Medium (MEM) Alpha (Sigma-Aldrich). All media were supplemented with 1% (v/v) antibiotics-antimycotic (Gibco) and 10 % (v/v) foetal calf serum (FCS) (HyClone).

The SAT2 viruses, ZIM/5/83 and ZIM/14/90, were obtained from the FMD World Reference Laboratory at the Pirbright Institute, Pirbright, UK. The ZIM/7/83 virus was obtained from the virus bank at the Transboundary Animal Diseases section (TAD) of the Agricultural Research Council, Onderstepoort Veterinary Institute (ARC-OVI) of South Africa. The SAT2/ZIM/14/90, SAT/ZIM/5/83 and SAT2/ZIM/7/83 viruses have been isolated from infected cattle and their origins have been described in Maree et al. (2011) and the passage histories are summarised in Table 1. Virus stocks were prepared and titrated using plaque assays in BHK-21, IB-RS-2, ZZ-R 127 or CHO monolayer cells as described by Rieder et al. (1993). Briefly, plaque assays were performed in triplicate by infecting monolayer cells in 35-mm cell culture plates (Nunc™) with the respective viruses for 1 h, followed by the addition of a 2 ml tragacanth overlay and incubation at 37 °C for 48 h. The infected monolayers were stained with 1% (w/v) methylene blue in 10 % (v/v) ethanol and 10 % (v/v) formaldehyde in phosphate-buffered saline (PBS), pH 7.4. Virus titres were expressed as the logarithm of the plaque forming units (PFU)/ml and plaque sizes defined as micro (<1 mm), small (S) (1–2 mm), medium (M) (3–5 mm) or large (L) (>5 mm), as described previously (Opperman et al., 2014).

2.2. Growth kinetics

One-step growth kinetic analyses were performed in BHK-21 cells. Briefly, BHK-21 cells were infected with virus for 1 h at a multiplicity of infection (MOI) of 2 and then washed with MBS-buffer (25 mM morpholine-ethanesulfonic acid (MES), 145 mM NaCl, pH 5.5), followed by addition of 3 ml virus growth medium (VGM) consisting of Eagle's basal medium (BME) containing 1% foetal calf serum (v/v) and 25 mM HEPES. The infected cells were incubated at 37 °C with 5% CO_2 influx. The infected cells were harvested at 2, 4, 6, 10, 12, 16 and 22 h post-infection (hpi) and subsequently frozen in VGM at −70 °C. Virus titres were determined using plaque assays and expressed as the logarithm of the PFU/ml.

2.3. Pathogenicity of SAT2 viruses in cattle

All animal work was approved and conducted according to the requirements of the OVI Animal Ethics Committee (AEC6.12) following national and international guidelines and the

Department of Agriculture, Forestry and Fisheries (DAFF, South Africa) Section 20 permit (03/07/2012). Cattle were housed in the biosafety level 3 isolation facility at TAD of the ARC-OVI.

Six FMD-seronegative Nguni calves, 6–12 months of age and *ca.* 150 kg, were divided randomly into three groups of two animals each and were housed in separate rooms. Each calf was inoculated intra-dermolingually with 1 ml of 10^5 Median Tissue Culture Infectious Dose ($TCID_{50}$) of cell-cultured ZIM/5/83 or ZIM/7/83 or 1 ml of 10^4 $TCID_{50}$ ZIM/14/90 virus divided into three tracks. The animals were monitored daily for signs of clinical disease (including elevated rectal temperatures, salivation and appearance of vesicles in the mouth and on the feet) for a period of 10 days. Rectal temperatures of 39.5–40.5 °C and >40.5 °C were considered as mild and severe fever, respectively. Clinical observations of FMD generalisation to sites other than the site of inoculation were scored daily as follows: mild fever or congestion or healing vesicle = 1; severe fever or vesicles = 2; severe lesions (including heel detachment or equivalent) = 3. The maximum clinical score per animal is 15 if severe fever and severe lesions are present on all four hoofs and the mouth other than the site of inoculation. Blood samples were collected every second day and analysed for the presence of anti-SAT2 antibodies using a serotype-specific blocking ELISA. The viral RNA from heparinised blood was detected using a two-step real-time RT-PCR assay according to the method described by Callahan et al. (2002).

2.4. Viral RNA extraction, cDNA synthesis, RT-PCR and sequencing

To obtain the open reading frame (ORF) nucleotide sequence of SAT2 viruses, total RNA was extracted from infected cell lysates using TRIzol® reagent (Life Technologies) according to the manufacturer's specifications and used as template for cDNA synthesis. Viral cDNA was synthesised using SuperScript III™ (Life Technologies) and either oligonucleotide primer 2B (5′- GACATGTCCTCCTGCATCTG) (Vangrysperre and De Clercq, 1996) or a modified oligo-dT primer (5′−CCATGGCGGCCGCTTTTTTTTTTTTTTTGGA). Amplification of cDNA copies of the *ca*. 3.0 kb Leader/capsid-coding region of the viral isolates was obtained by PCR using Expand Long Template Taq DNA polymerase™ (Roche) with specific oligonucleotides (NCR2: 5′-GCTTCTATGCCTGAATAGG and WDA: 5′-GAAGGGCCCAGGGTTGGACTC) following the manufacturer's recommendations. The P2/P3 non-structural protein-coding region was amplified using the modified oligo-dT oligonucleotide and a VP1-specific oligonucleotide (5′-GAGTCCAACCCTGGGCCCTTCTTCTTC). Direct DNA sequencing of the amplicons was performed using the ABI PRISM™ BigDye Terminator Cycle Sequencing Ready Reaction Kit v3.0 (Perkin Elmer Applied Biosystems). The consensus ORF nucleotide sequences were assembled with Sequencher 4.7 DNA sequence analysis software (Gene Codes Corporation, Ann Arbor, MI, USA) and compared to that of ZIM/7/83 (GenBank accession codes: JQ639289 and DQ009726) or EGY/09/12 (JX014255) or ZIM/14/90 (GenBank accession codes: DQ009728 and KJ144910). The GeneBank accession codes for ZIM/5/83 are JQ639289 and AF540910.

2.5. Pyrosequencing

To determine the population of sequence variants present in the ZIM/5/83 and ZIM/7/83 viruses, the outer-capsid coding region was amplified from cDNA as ten overlapping fragments of 400 bp each using virus-specific fusion oligonucleotides. The fusion

oligonucleotides included a 19-mer adapter sequence at the 5′-end, a 4-bp tag sequence of "ACGT" and a 3′-end of 22–28 nucleotides complimentary to the ZIM/7/83 genome. PCR was performed using the Expand Long Template system (Roche Diagnostics) with added *Pfu* DNA polymerase (Promega). PCR reactions consisted of 30 cycles of denaturation at 95 °C for 20 s, annealing at 56 °C for 20 s and extension at 68 °C for 3 min, with a final extension step at 68 °C for 7 min. The purified PCR products were nebulized, clonally amplified on capture beads in water-in-oil emulsion micro-reactors at predetermined DNA copies per bead using oligonucleotides complimentary to the adapter sequence of the fusion oligonucleotides. The sequencing run was performed using the GS FLX instrument (Roche, 454 Life Sciences, Branford, CT, USA) at Inqaba Biotech™, Pretoria, South Africa.

Low-quality reads were removed and the remaining sequences were built into a multi-sequence assembly using the CLC Genomic Workbench (CLC bio) computer software package. The frequency of nucleotide substitutions or single nucleotide variances (SNV) detected between ZIM/5/83 or ZIM/7/83 sequence data reads and the respective reference sequences were calculated using CLC Genomic Workbench 8.0.1 (CLC Bio, Aarhus, Denmark). The nucleotide sequences were also translated into protein sequences and the single residue variances (SRV) calculated.

2.6. Construction of chimeric full genome infectious clones, transfection and virus recovery

To investigate the growth, virulence, antigenic and stability properties relating to the P1 region of the SAT2/EGY/9/12 virus, a capsid-coding exchange strategy using the pSAT2 genome-length cDNA clone (van Rensburg et al., 2004) was used in the construction of a chimeric SAT2 clone. A synthetic sequence (GeneScript) of the EGY/09/12 outer capsid (VP2, VP3 and VP1) and 2A protein coding regions (Valdazo-González et al., 2012; GenBank Accession no. JX014255) was PCR amplified using the Advantage® 2 PCR Enzyme System (Clontech), and genome-specific sense (5′-*GCTCGAGGACCGAATATT*GACCACGCGTCACGGGACCACGA) and anti-sense (5′-*AAGAAGAAGGGCCCGGGG*TTGGACTCAACGTCTCCAGCCAA) primers. The primers contained 5′-end 18 nt overhangs complimentary to the plasmid (indicated in italics) and 3′-end 23 nt overhangs complimentary to the donor EGY/9/12 sequence. Insertion of the outer capsid of EGY/9/12 into the corresponding region of pSAT2 was performed using the In-Fusion® HD Cloning Kit (Clontech) to generate p^{EGY}SAT2. The nucleotide sequences of the inserted regions were subsequently determined to verify ORF integrity.

Similarly, the effect of different replicated genomes in the SAT2/ZIM/7/83 population in a defined genetic background was investigated by obtaining outer capsid-coding regions of the SAT2/ZIM/7/83 cDNA through PCR amplification with genome-specific oligonucleotides. Unique *Ssp*I and *Xma*I sites were introduced at the 5′ and 3′ termini of the 2.2 kb amplicons, respectively, to facilitate insertion into the pSAT2 plasmid. Following ligation, transformation and clonal expansion, recombinant plasmids were selected and sequenced. A total of 21 clones were sequenced and only one recombinant had five nucleotide differences in the outer capsid-coding region. The recombinant clone was labelled as $pSAT2^{SNV}$ and used for transfection.

RNA was synthesised from *Swa*I-linearised genome-length plasmid DNA, p^{EGY}SAT2 and $pSAT2^{SNV}$, using the MEGAscript™ T7 kit (Ambion) as described by Opperman et al., 2012. The *Swa*I restriction enzyme site is located downstream of the poly(A) tract of the SAT2

genome-length clone. BHK-21 cell monolayers, in 35-mm diameter cell culture plates (Nunc™), were transfected with the *in vitro*-generated RNA (2−3 μg) using Lipofectamine2000™ (Life Technologies) according to the manufacturer's instructions. The transfection medium was removed after 5 h and replaced with Eagle's basal medium (BME) containing 1% FCS, followed by incubation for 48 h at 37 °C with 5% CO_2 influx. Viruses were subsequently harvested from the transfected cells following a freeze–thaw cycle and the transfection supernatants were used for four serial passages on BHK-21 cells until complete CPE was obtained. Viruses recovered from BHK-21 cells transfected with p^{EGY}SAT2 or $pSAT2^{SNV}$ were designated v^{EGY}SAT2 or $vSAT2^{SNV}$, respectively.

2.7. Structural analysis of variable amino acids in capsid subunits

Three-dimensional models of the capsid proteins VP1, VP2, VP3 and VP4, as a pentamer of the SAT2 viruses, were constructed based on the crystallographic coordinates of $A_{10}61$ (1ZBE) (Fry et al., 2005). The models were based on an optimal alignment of the capsid proteins, performed with ClustalX software (Thompson et al., 1997) using the default parameter settings. Structures were visualised with PyMol v0.98 (Schrödinger, LLC, New York, NY).

2.8. Virus purification and capsid stability assays

To prepare purified virus, culture fluids from infected BHK-21 cells were harvested, clarified by centrifugation, concentrated with 8% (w/v) PEG-8000 and resolved on 10 %–50 % (w/v) sucrose density gradients (SDG) using rate zonal centrifugation for 16 h at 36,000 *g* and 4 °C (Knipe et al., 1997). The gradients were fractionated, analysed spectrophotometrically at an OD_{259nm} and the fractions with 146S virions, calculated using the extinction coefficient E_{259nm} = 78.8 (Doel and Mowat, 1985), were pooled for analysis. The presence of the outer capsid proteins were verified using SDS-polyacrylamide gel electrophoresis (SDS-PAGE) and the integrity of the RNA verified by RT-PCR and sequencing of the VP1-coding region, as described above.

The pH dissociation assay was performed as described by Knipe et al. (1997). Briefly, 9×10^6 to 5×10^7 SDG-purified infectious virus particles were mixed 1:50 with TNE buffers [100 mM Tris (pKa = 8.0 at 25 °C), 10 mM EDTA, 150 mM NaCl] ranging from pH 7.4, 6.5 and 6.3 for 30 min at 25 °C. For pH ranges of 5.8–6.2, the virus particles were mixed 1:50 with MES buffers [100 mM MES (pKa = 6.1 at 25 °C), 10 mM EDTA, 150 mM NaCl] of pH 5.8, 6.0 and 6.2. Virus particles were also mixed with VGM (supplemented with 1% FCS and 40 mM HEPES) as a control. The samples were subsequently neutralised with 1 M Tris (pH 7.6), 150 mM NaCl and titrated using plaque assays in BHK-21 cells (section 2.1). The average titres for each virus for each pH treatment from two independent inactivation experiment were used to calculate the percentage of remaining infectious particle using the average titre at pH 7.4 as denominator. The pH_{50} was calculated as the pH value where the virus titre is halfway between the highest and lowest titre within the pH range 7.4–5.8 (Curry et al., 1995).

A thermostability assay was performed by treating aliquots of the virus particles diluted 1:50 in TNE buffer (pH 7.6) at temperatures of 4 °C, 25 °C, 37 °C, 45 °C or 55 °C for 30 min, followed by cooling on ice and titration on BHK-21 cells. The 1:50 dilution of the SDG-purified particles in all of the above assays ensured that the stabilising effect of sucrose was negligible, as it was calculated from the viscosity to be less than 1% in the final dilution. The

experimental groups at each pH or temperature treatment were compared using one-way ANOVA 2-factor repeated measures, followed by a Bonferroni multiple comparisons test. The confidence interval was 95 %. Statistical analyses were carried out using GraphPad Prism v5.0 (GraphPad Software).

2.9. Indirect ELISA using SAT2-specific soluble single chain variable fragments (scFvs)

An indirect ELISA was used to determine the reactivity of the ZIM/7/83 and vSAT2^{SNV} viruses utilising three unique SAT2-specific scFvs, as described by Opperman et al. (2012). Briefly, ELISA plates were coated with 30 µg/ml of SDG-purified virus, diluted in 1 × PBS, as well as with 2% (w/v) casein in 1 × PBS as a negative control. Following incubation overnight at 4 °C, all ELISA plates were washed with 1 × PBS containing 0.05 % (v/v) Tween-20 and affinity-purified soluble scFvs (5−10 µg/ml) in 1 × PBS containing 2% (w/v) casein, were added. Soluble scFvs were detected using an anti-c-Myc MAb 9E10, expressed from the murine hybridoma Mycl-9E10 (CAMR, UK), and polyclonal rabbit anti-mouse IgG conjugated to horseradish peroxidase (P0260; Dako).

2.10. Virus growth competition assay

Monolayers of BKH-21 and ZZ-R 127 cells in 25-cm^3 tissue culture flasks were either infected with v^{EGY}SAT2 or vSAT2 viruses or co-infected with both viruses simultaneously at different MOIs. Co-infection with vSAT2 and v^{EGY}SAT2 and were at MOI ratio of >1:10 for each cell line. Complete cell death was observed within 24 h and 10 % of the supernatant was used to infect a fresh monolayer for up to ten passages. Each assay was performed using three repeats. Viruses were subsequently harvested from infected cells by a freeze-thaw cycle, followed by RNA extraction utilising a guanidine-based QIAamp® Viral RNA kit (Qiagen) and used as template in quantitative RT-PCR described below.

2.11. Quantitative RT-PCR

A set of primers and probes were designed and synthesised (TIB Molbiol, Berlin) to specifically detect the capsid coding region of ZIM/7/83 (AF540910) (ZIM-F: 5′-AGATTCACCCATGTTCTGACAAA and ZIM-R: 5′-GTTCGTGTTCGCCAAGG) and EGY/9/12 (JX014255) (EGY-F: 5′-CAGCCTAAACTACCACTTCATGTAC and EGY-R: 5′-CACTGCGAACGAGAAAGAAG). The probes (EGY-P: 5′-TTGACCAGATGCCTAGCACACCG and ZIM-P: 5′-AGGGTCTTCTCGTTGGTGTCCAT) were modified with fluorescent dye 6-carboxyfluorescein (FAM) and quencher BlackBerry® Quencher (BBQ), respectively. The quantitative PCRs were performed separately for each virus. Duplicates of extracted viral RNA from the co-infection experiment were used as template for cDNA synthesis using the SuperScript® III One-Step RT-PCR System with Platinum® *Taq* DNA Polymerase (Invitrogen), followed by amplification in a single reaction. One cycle of cDNA synthesis was performed at 50 °C for 20 min, followed by PCR amplification of 94 °C for 2 min, 40 cycles at 94 °C for 15 s and 67 °C (vSAT2) or 69 °C (v^{EGY}SAT2) for 30 s. The quantitative RT-PCR was performed and data analysed using the CFX96 PCR-cycler and CFX Manager Software V 2.0 (Bio-Rad).

Absolute quantification standards of pSAT2 and p^{EGY}SAT2 were prepared from *in vitro*-transcribed RNA, followed by removal of residual DNA with DNase I (Invitrogen). RNA concentrations were determined spectrophotometrically and a ten-fold serial dilution was

prepared from 1×10^{10} to 1×10^{3} copies/µl of RNA transcript in total cellular RNA extracted from virus-free BHK-21 cells. Each standard RNA sample was tested in triplicate. The copy number of the standard RNA molecules was calculated using the formula described by Whelan et al. (2003)., *i.e.* (X g/µl RNA/[transcript length in nucleotides x 340]) x 6.022×10^{23} = Y molecules/µl.

The average copy number for each virus was determined from the Ct values of the duplicate samples. Two biological replicates of each treatment were averaged and their standard deviations determined. The data was analysed through repeated measures of ANOVA with Bonferroni adjustment of *P*-values for post-hoc comparisons. All statistical analyses were performed using GraphPad Prism v5.03 (GraphPad Software, Inc.).

3. Results

An infectious genome-length clone (pSAT2) of the SAT2/ZIM/7/83 virus has been constructed and characterised previously (van Rensburg et al., 2004). We have exchanged the capsid-coding region of the SAT2 genome-length clone with the corresponding region of SAT2/EGY/9/12 (GenBank accession number JX570622), responsible for a 50 % mortality rate in cattle (Ahmed et al., 2012). The recovered virus was designated v^{EGY} SAT2. We have used the SAT2 viruses ZIM/5/83 (BTY4), its derivative ZIM/7/83 (B1 BHK5B1BHK4) or v SAT2, ZIM/14/90 (BTY1RS3), and v^{EGY} SAT2 (BHK5) in cell binding and infectivity assays, virus fitness, pathogenesis studies in cattle, genome sequence comparisons and stability of capsids to determine virus factors involved in virulence *in vitro* and *in vivo*.

3.1. Clinically SAT2 viruses cause mild to severe infections in cattle

The pathogenesis of EGY/9/12 has been reported elsewhere to induce multiple clinical signs in approximately 70 % of bovidae and 94 % mortality among calves (Zaher et al., 2014). To determine the pathogenesis of the ZIM/5/83, ZIM/7/83 and ZIM/14/90 viruses in cattle, the viruses were inoculated into the tongues of calves. Clinical examination of the calves was performed on a daily basis and blood samples were collected to determine antibody responses and viraemia (Fig. 1).

Calves (1124 and 1130) inoculated with 10^4 $TCID_{50}$ of the ZIM/14/90 virus exhibited FMD clinical signs one-day post-inoculation (dpi), which included elevated temperatures (> 40.5 °C) and vesicles at the sites of inoculation (Fig. 1A). Calf 1130 had severe tongue lesions that spread beyond the site of inoculation. At 2 dpi the virus had spread systemically and vesicles or severe lesions developed on the feet of both calves. Clinical signs peaked with severe lesions being observed on all four feet 3 dpi (Fig. 1A). Lesions were still present until 8 dpi but thereafter started to heal. Analysis of the sera from these calves showed the early presence of anti-SAT2 antibodies from 3 or 4 dpi. Both animals seroconverted 6 dpi with a $\log_{10}$ titre of >1.8 and diagnostic threshold titres were reached between 9–11 dpi. No virus could be isolated from whole blood; however, FMDV RNA was detected using real-time RT-PCR. The Ct values increased gradually, indicative of decreasing viral RNA levels (21.5–36.0 for 1124 and 28.0–35.6 for 1130) from 2 to 7 dpi together with the increase in antibody titres (Fig. 1A).

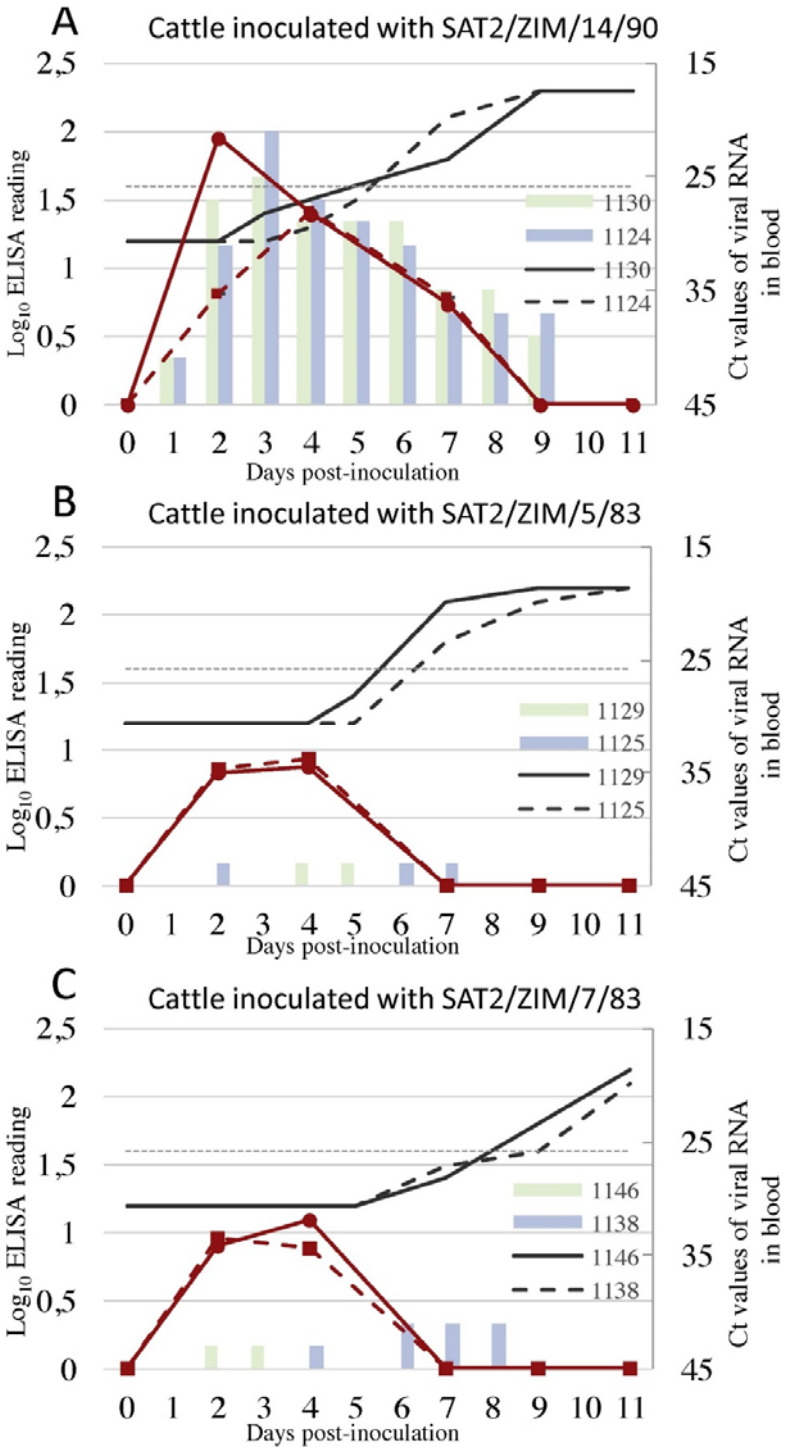

Fig. 1. Pathogenesis of SAT2 viruses in cattle through clinical observation post- inoculation (0 to 21 dpi). The relationship between detection of FMDV RNA in blood by qRT-PCR (red lines) and the presence of anti-SAT2 FMDV antibodies (black lines) in the context of clinical score of cattle intra-dermolingually inoculated with with ZIM/14/90 (A), ZIM/5/83 (B) and ZIM/7/83 (C). The clinical scores were calculated as described in Materials and Methods, 0-12 indicating low to high severity (score of 0-12 scaled to fit on the 0-2 y-axis). Blood samples were collected and the serum was analysed for the presence of anti-SAT2 FMDV antibodies in a liquid-phase blocking ELISA and for the presence of FMDV RNA by qRT-PCR (Ct value is the mean of two animals). The data for two animals inoculated with ZIM/14/90 (A), ZIM/5/83 (B) or ZIM/7/83 (C) are shown. The dashed horizontal line is set at 1.6 $\log_{10}$ antibody titre and indicates the diagnostic cut-off level in the ELISA

The ZIM/5/83 and ZIM/7/83 viruses were also used to inoculate two calves each, introducing an aggregate dose each of approximately 10^5 $TCID_{50}$, ten times the aggregate dose for ZIM/14/90. Both animals (1125 and 1129) inoculated with ZIM/5/83 developed mild clinical signs 2 dpi, which included mild elevated temperatures (39.5–40 °C) and tongue vesicles at the site of inoculation (Fig. 1B). No systemic spread or lesions on the feet were observed. However, analysis of the sera showed the presence of anti-SAT2 antibodies with log_{10} titre of 1.4 from 5 dpi (1129) (Fig. 1B). Similarly, the two calves (1146 and 1138) inoculated with ZIM/7/83 developed mild elevated temperatures and a vesicle at the site of inoculation which subsequently healed. Only calf 1138 developed small vesicles on the left front foot and right hind foot 6–8 dpi, thereafter the lesions started to heal (Fig. 1C). No other evidence for systemic spread of virus was visible. Analysis of the sera showed an increase in anti-SAT2 antibodies from 7 dpi (Fig. 1C). Neither ZIM/5/83 nor ZIM/7/83 virus could be isolated from whole blood up to 11 dpi. FMDV RNA was detected (Ct values < 40) between 2–5 dpi for both calves infected with ZIM/5/83 (Fig. 1B) and ZIM/7/83 (Fig. 1C).

3.2. SAT2 viruses differ in their relative infectivity, growth properties and virulence in cultured cells

The cytopathic effect (CPE) produced by the SAT2 viruses on BHK-21 cells differed when viewed by light microscopy. Although ZIM/7/83 was derived from ZIM/5/83, cells infected with ZIM/7/83 caused complete lysis and detachment of more than 95 % of the cells within 8−16 hpi, whereas cells infected with ZIM/5/83 or ZIM/14/90 never achieved complete CPE, even after 48 hpi (Table 1). Cells infected with v^{EGY}SAT2 detached completely at 24 hpi and the results were identical to those reported for the EGY/9/12 virus in BHK-21 cells (Zaher et al., 2014).

Table 1
A summary of the SAT2 viruses and the recombinant or chimeric derivate, the passage histories, virus titres on different cell lines and properties in cell culture.

Virus[a]	Passage history[b]	Titre (PFU/ml) in the following cell line						Plaque phenotype on BHK-21 cells[c]	CPE on BHK-21 cells (hpi)[e]
		BHK-21	ZZ-R 127	CHO-K1	CHO-677	CHO-745	CHO-lec2		
SAT2/ZIM/5/83	BTY4	2.0×10^5	n.d.[d]	0	0	0	0	Large	> 48
SAT2/ZIM/5/83	BTY4BHK8	3.4×10^7	n.d.	6.0×10^6	0	0	n.d.	Medium	42-48
SAT2/ZIM/7/83	B1BHK5B1BHK4	5.6×10^8	n.d.	3.0×10^6	0	0	7.6×10^6	Medium, large	8-16
SAT2/ZIM/14/90	BTY1RS3BHK8	4.0×10^6	n.d.	0	0	0	0	Large	42-48
vSAT2	BHK5	2.4×10^7	5.8×10^8	1.2×10^6	6.0×10^6	1.6×10^6	7.6×10^6	Small, medium, large	8-16
v^{EGY}SAT2	BHK5	2.5×10^6	2.3×10^7	1.7×10^3	0	0	8.0×10^5	Micro, small	24

[a] The viruses vSAT2 and v^{EGY}SAT2 were produced following transfection of BHK-21 cells with RNA produced from the genome-length clones pSAT2 and p^{EGY}SAT2, and five recovery passages in BHK-21 cells.
[b] The passage history of the SAT2 viruses and their derivates are indicated by cell type, followed by the number of passages: B = bovine; BTY = bovine thyroid cells; RS = IB-RS-2 cells; BHK = baby hamster kidney cells (strain 21, clone 13).
[c] Plaque morphologies were obtained using monolayers of BHK-21 cells infected with the indicated viruses with a tragacanth overlay for 40 h prior to staining with 1% methylene blue. Plaques for SAT2 viruses are generally large (> 5 mm) with opaque edges, but serial passage in cultured BHK-21 cells is accompanied by small (1−2 mm) to medium (3−5 mm) plaques and clear edges. v^{EGY}SAT2 produced characteristic micro- (< 1 mm) to small-sized plaques on BHK-21 cells.
[d] n.d. = not done.
[e] hpi = hours post infection.

The ZIM/5/83 (BTY4) and ZIM/14/90 (BTY1RS3BHK8) viruses produced large plaques (>5 mm) on BHK-21 cells and did not infect CHO-K1 cells, but after eight passages in BHK-21 cells the ZIM/5/83 (BTY4BHK8) virus yielded an increased number of medium-sized plaques (3−5 mm) (Table 1). The titre of ZIM/5/83 in BHK-21 cells increased from 2.0×10^5 to 3.4×10^7 PFU/ml (a 2× log_{10} increase) and infected and replicated in CHO-K1 (wild-type, glycosaminoglycan positive) cells (6×10^6 PFU/ml), following eight passages on BHK-21 cells. The ZIM/7/83 virus produced large and medium plaques on BHK-21 cells, was able to propagate in CHO-K1 and CHO-lec2 (sialic acid-deficient) cells and attained an average titre of 5.6×10^8 PFU/ml in BHK-21 cells, which was approximately 2 × log_{10} higher than the titre attained in CHO-K1 cells (3×10^6 PFU/ml). The v^{EGY}SAT2 virus produced micro-sized

plaques (<1 mm) on BHK-21 cells. This plaque phenotype was distinctly different from the plaques produced by the other SAT2 viruses, suggesting dissimilarities either in the cell entry mechanism or in the rate of virus replication. The v^{EGY}SAT2 virus was also able to infect and replicate in CHO-K1 and CHO-lec2 cells; however, the highest titres were observed in BHK-21 cells, followed by CHO-lec2 cells and 1,000-fold lower titres in CHO-K1 cells (1.7×10^3 PFU/ml). No growth was observed on CHO-677 (heparan sulfate or HS-deficient cell line) and CHO-745 (HS and chondroitin sulfate -deficient cell line) cells for ZIM/5/83, ZIM/7/83, ZIM/14/90 or v^{EGY}SAT2, indicating that none of the SAT2 viruses were able to infect and replicate in these cell lines. However, for the first time, we have observed the ability of vSAT2 to infect and replicate in CHO-677 and CHO-745 cells, suggesting it may utilise a different and yet unknown receptor for cell entry. On ZZ-R 127 cells, a goat cell line known to express $\alpha_v\beta_6$-integrin receptors (Brehm et al., 2009), v^{EGY}SAT2 and vSAT2 produced more than a ten-fold higher infectivity titre compared to titres attained in BHK-21 cells (Table 1).

The growth kinetics of the ZIM/5/83, ZIM/7/83, ZIM/14/90 and v^{EGY}SAT2 viruses were compared in BHK-21 cells (Fig. 2). The results indicated that the growth kinetics of the ZIM/5/83 virus was similar to ZIM/7/83 and ZIM/14/90, regardless of differences observed in CPE and relative infectivity titres. The titre of the v^{EGY}SAT2 virus was found to be 10-fold lower than the ZIM/7/83 virus titres at 8–22 hpi. Real-time monitoring of the growth of ZIM/5/83 and ZIM/7/83 in BHK-21 cultured cells revealed that at 37 °C the virus-induced cytolysis, the cause of CPE, was detected as early as 8.5 and 6 hpi, respectively, at 2×10^4 PFU per well (Fig. S1). A rapid decline of the cell index (CI) followed for ZIM/7/83- and ZIM/5/83-infected cells, which decreased by 50 % within 9 and 14 hpi, respectively, at a titre of 4.3 $\log_{10}$.

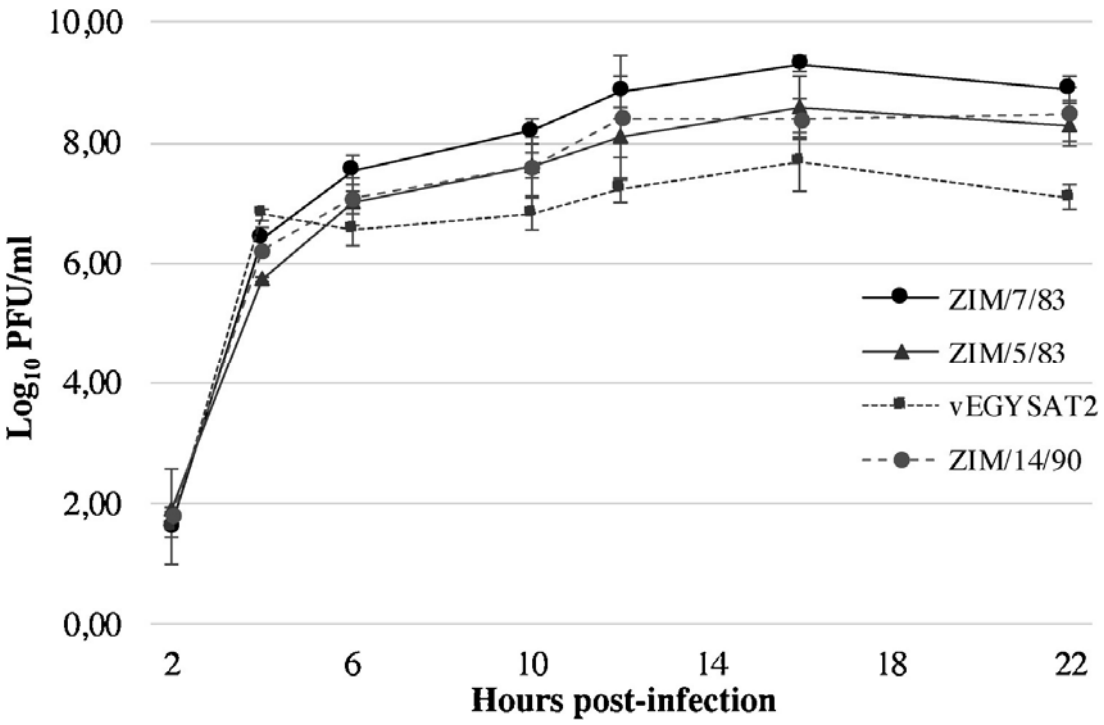

Fig. 2. One-step growth kinetic studies performed in BHK-21 cells. The relative release of virus particles from cells infected with the ZIM/7/83, ZIM/14/90, ZIM/5/83 and v^{EGY}SAT2 viruses are shown as the means $\log_{10}$ virus titers ± standard deviations at different times post-infection as indicated in the graph. The results are from quadruple wells.

Taken together, the replication dynamics indicate that ZIM/7/83 virus can infect and replicate more effectively in cultured cells compared to the other SAT2 viruses, while the replication of v^{EGY}SAT2 was distinctly different and its growth kinetics was delayed in BHK-21 cells.

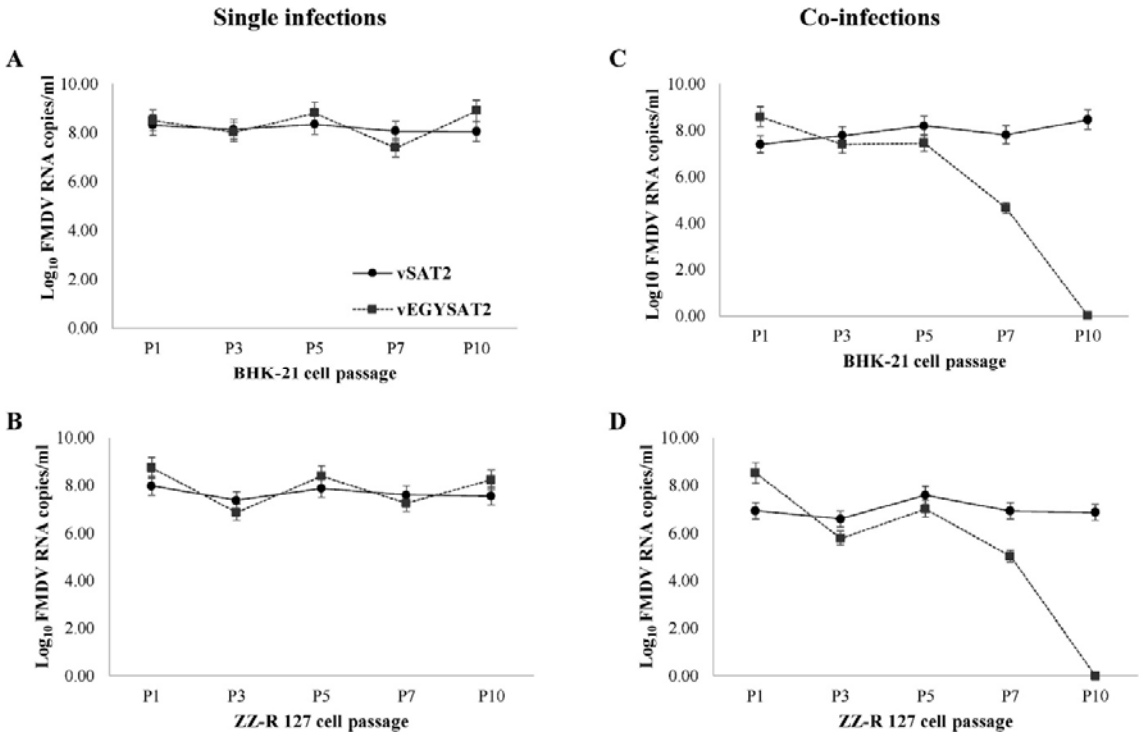

Fig. 3. Virus replicative fitness of the vSAT2 and v^{EGY}SAT2 viruses assessed in a co-infection assay in BHK-21 and ZZ-R 127 cells. The results are shown as the RNA copies/ml and are presented as means ± standard deviations of three independent experiments. Graphs A and B depict the results of single infections of BHK-21 and ZZ-R 127 cells, respectively, with vSAT2 and v^{EGY}SAT2. Graphs C and D depict the results of cells co-infected with vSAT2:v^{EGY}SAT2 at a MOI ratio of >1:10.

3.3. The ZIM/7/83 derivative, vSAT2, outcompetes v^{EGY}SAT2 in cultured cells despite pathogenic and virulence differences

Next, we assessed the *in vitro* relative replicative fitness of the two genetically and biologically disparate viruses, vSAT2 and v^{EGY}SAT2. The two viruses were used to infect cultured cells individually or co-infect cells at an MOI ratio of > 1:10 (vSAT2:v^{EGY}SAT2), followed by ten serial passages. The mean and standard deviation of the acquired RNA copy number/µl were calculated for each passage and the results expressed as $\log_{10}$ viral copies/ml (Fig. 3). BHK-21 and ZZ-R 127 cells infected with either vSAT2 or v^{EGY}SAT2 showed stable replication of the two viruses throughout ten serial passages with viral RNA copies ranging from 1.2×10^7 to 6.0×10^8 throughout propagation (Figs. 3A and 3B). Co-infection with vSAT2 and v^{EGY}SAT2, at an MOI ratio of >1:10, resulted in an initial v^{EGY}SAT2 RNA concentration (passage 1) of 10× and 100× more than vSAT2 in BHK-21 and ZZ-R 127 cells, respectively. Despite the v^{EGY}SAT2 advantage, the co-infection resulted in a significant reduction ($P < 0.001$) in RNA copies of v^{EGY}SAT2 from passage five onwards (Figs. 3C and 3D). No v^{EGY}SAT2 RNA could be detected at passage ten in either BHK-21 or ZZ-R 127 cells. The vSAT2 virus retained a high number of viral RNA copies throughout all passages in both BHK-21 and ZZ-R 127 cells (Figs. 3C-3D). The data suggests that although both vSAT2 and v^{EGY}SAT2 are able to infect and replicate in BHK-21 and ZZ-R 127 cells

individually, vSAT2 outcompeted v^{EGY}SAT2 in both cell lines and RNA copy numbers of v^{EGY}SAT2 were reduced gradually with each passage to below detectable levels of viral RNA by passage ten.

3.4. Common genetic variants within SAT2 virus populations contribute to the average population phenotype

Examination of the genome sequences of the SAT2 viruses revealed multiple sites of variation between the predominant virus populations, as could be expected from the genome of an RNA virus. At least 21.1 % nucleotide differences were observed in any pairwise alignment of the genomes of ZIM/7/83, ZIM/5/83 or ZIM/14/90 to the EGY/9/12 genome. The most variation was observed in the outer capsid-coding sequences. A pairwise alignment of the genomes of either ZIM/7/83 or ZIM/5/83 and ZIM/14/90 showed 8.4 % nucleotide differences. At least 39 nucleotide changes were detected across the genomes (7036 nt) of ZIM/5/83 and its derivative, ZIM/7/83, of which 18 were silent mutations and the remaining 21 resulted in amino acid changes.

The most variable outer capsid protein, VP1 (1D), had 51 (n = 214) variable amino acid residues in a complete alignment of the deduced amino acid sequences of the capsid proteins of ZIM/7/83, ZIM/5/83, ZIM/14/90 and EGY/9/12. The VP2 (1B) and VP3 (1C) capsid proteins displayed 19 and 29 variable residue positions in 219 and 222 residues, respectively. Variation was not random, but focused in local regions of variability (Fig. S2). The capsid proteins of the EGY/9/12 virus displayed unique residues: seven in VP2 (1B), 18 in VP3 (1C) and 27 in VP1 (1D), while ZIM/7/83 and ZIM/5/83 had a unique His residue at position 4 of VP4 (1A). The outer capsid proteins of ZIM/5/83 and ZIM/7/83 revealed six amino acid differences, four of which occurred in the VP1 (1D) protein and three were surface exposed. The most dramatic of these changes in terms of altering residue charge included E1160 K, Y1169H and E1212 K in ZIM/7/83. While only 2% of the 1397 amino acid residues of the ZIM/7/83, ZIM/5/83 and ZIM/14/90 non-structural proteins (NSPs) were variable, the variable residues increased to 13.8 % when EGY/9/12 NSPs were included in the comparison (data not shown). The Leader protease, 3A and 3B peptides were the most variable NSPs in our study with 40 %, 24.1 % and 22.5 % variable residue positions, respectively, and $3D^{pol}$ was the most conserved with only 9.6 % variable residues. Many mutations and deletions occur in the C-terminus of the 3A protein of FMDV. Previous reports demonstrated that 3A, but not 3B, plays a role in virulence and host range determination (Pacheco et al., 2003, 2010). In this regard, it is interesting to note that compared to the 3A protein of ZIM/7/83, the EGY/9/12 virus had a two-amino acid deletion at positions 128–129 and a two-amino acid insertion between residue positions 147-148. Deletions in this region of 3A have not been associated with virulence of FMDV (Pacheco et al., 2010).

FMDV exists as a quasispecies with different replicated genomes occurring in a virus population, each contributing to the average population phenotype. To compare the different replicated genomes in the ZIM/7/83 and ZIM/5/83 virus populations we applied two methods: (1) ultra-deep sequencing, based on the 454/Roche™ pyrosequencing technology, to detect low-frequency single nucleotide variants (SNVs) in the ZIM/5/83 and ZIM/7/83 virus populations and; (2) cloning of the outer capsid-coding region of ZIM/7/83 in the defined genetic background of the infectious cDNA clone, pSAT2.

PCR was used to amplify defined, overlapping outer capsid-coding regions and the amplicons were sequenced. The assembled reads had on average 87 (58–136) and 146 (48–167)-fold

coverage at each nucleotide position for ZIM/7/83 and ZIM/5/83, respectively, and were used to obtain the consensus sequence of each virus. Variable nucleotides and amino acids for the complete capsid-coding region were determined using the CLC Genomic Workbench (CLC bio) software. After correction for insertions and deletions at least 14.7 % (n = 326 nt) and 6.5 % (n = 144) SNVs were observed in the capsid-coding regions of ZIM/5/83 and ZIM/7/83, respectively, albeit the majority at very low frequency (Table 2). There were 19 and 10 SNVs with frequencies higher than 1% in each population, separating it from the effect of artificially (cDNA and PCR)-induced changes or pre-existing very low frequency SNVs. To separate synonymous versus non-synonymous changes, the deduced amino acid differences from the consensus sequences of high frequency variants of the parent populations were compared (Table 2). At least 22 and 12 of these SNVs translated into variable amino acid positions (n = 758) of the capsid proteins within the respective ZIM/5/83 and ZIM/7/83 populations. The VP1 (1D) protein of ZIM/5/83 displays an E1160, Y1169 and E1212 in >99 % of the population. However, the ZIM/7/83 VP1 (1D) had E1160 K and E1212 K amino acid substitutions in 100 % and 95 % of the population, respectively, whilst Y1169H was observed at a frequency below the cut-off value of 1%.

Table 2
Summary of the single nucleotide variance frequency and amino acid changes within the SAT2 virus populations of ZIM/5/83 and ZIM/7/83.

Coding region[a]	Nucleotide	SAT2/ZIM/5/83[d]			SAT2/ZIM/7/83[e]			Amino acid position[b]
		Nucleotide[c]	*Frequency (%)*	*Amino acid*	*Nucleotide*[c]	*Frequency (%)*	*Amino acid*	
1A(VP4)	13	T→C	1.34	S→P	T	–	S	4005
	14	C	–	S	C→T	3.03	S→L	4005
	27	A	–	T	A→G	2.02	T→A	4009
	32	C→T	1.35	S→L	C→T	< 1	S→L	4011
	109	C→G	4.48	Q→R	C	–	Q	4037
	117	C→T	1.01	G	C	–	G	4039
	121	A→G/T	1.35	N→D/S	A	–	N	4041
	141	C→T	1.37	S	C	–	S	4047
	205/6	T→A	< 1	S→P/F	T→A	3.03	S→Y/Q	4069
1B (VP2)	449	A→G	2.08	K→R	A→G	2.00	K→G	2065
	450	G→T	2.08	L→S	G→T	2.00	L→S	2066
	523	A→G	3.12	T→V	A	–	T	2090
	607	G	–	G	G→C	4.04	G→A/R	2118
	676	T→C	3.33	S→P	T	–	S	2141
	873	A	–	P	A→C	1.38	P	2206
1C (VP3)	1301	A→G	1.13	E→G	A	–	E	3130
	1309	A→G	1.13	R→G	A	–	R	3133
	1347	C→T	1.15	Y	C	–	Y	3145
	1379	A→C	2.08	Q→P	A	–	Q	3156
	1392	C→T	1.04	A→V	C	–	A	3160
	1443	C→G	1.20	A→P	C	–	A	3178
	1444	G→C	1.20	A→P	G	–	A	3178
	1536	A→G	1.44	G	A	–	G	3208
1D (VP1)	1607	T→G	1.77	V→G	T	–	V	1010
	1731	T→C	2.46	V	T	–	V	1051
	*1769/70***	*CG*	*100*	*A*	*GC*	*100*	*G*	*1064*
	*1856***	*G*	*100*	*G*	*G→A*	< 1	*G→E*	*1093*
	1886	A→C	< 1	N→T	A→C	2.04	N→T	1103
	1892	T→C	1.37	M→T*	T	–	M	1105
	1897	T→G	1.37	F→V	T	–	F	1107
	1900/1	TC→CT	3.20	S→L*	TC→CT	1.96	S→L	1108
		T→G	1.37	F→L	T	–	F	1115
	2056	G	100	E	A→G	100	E→K	1160
	2083	T→C	< 1	Y→H	T	100	Y	1169
	2106	C→G	1.14	V	C	–	V	1176
	2212	G	100	E	G→A	94.94	E→K	1212

[a] The capsid coding region (P1) is 2220 nucleotides in length and encode a 741 amino acid polypeptide.
[b] The amino acid residues have been numbered independently for each protein. For each residue, the first digit indicates the capsid protein (VP1, VP2, VP3 or VP4) and the last three digits the amino acid position in SAT2/ZIM/5/83 and SAT2/ZIM/7/83 P1 polypeptide sequence.
[c] The '- 'indicates no single nucleotide variation was observed at that position.
[d] GenBank Accession no. JQ639289 and AF540910.
[e] GenBank Accession no. AF540910 and DQ009726.
* The M1105→T and S→L were the only two substitutions linked in a sequenced fragment and was present at a frequency of 1.37 in the genome.
** The nucleotide changes at positions 1769/70 and 1856 was observed in a clone of SAT2/ZIM/7/83. These changes were also accompanied with changes at nucleotide positions 2083 and 2212.

Next, we inserted amplicons of the ZIM/7/83 capsid-coding region into the pSAT2 plasmid and the linearized DNA was used as templates for the synthesis of full-length RNA. The transcripts were transfected into BHK-21 cells and viable viruses selected. Plaque

morphology and outer capsid protein sequences of 21 recombinant viruses were identical to the consensus sequence of ZIM/7/83. However, sequencing revealed one recombinant virus, designated vSAT2^{SNV}, with five nucleotide differences compared to vSAT2 (G1647A, G1769C, G1856A, C2083 T and G2212A). The deduced amino acid sequences showed that the nucleotide differences translated into four amino acid substitutions (G1064A, G1093E, H1169Y and K1212E) in the VP1 (1D) protein between vSAT2^{SNV} and ZIM/7/83 (Table 3). The two residues A1064 and Y1169 were identical to that of ZIM/5/83. The G1093E and E1212 K mutations would lead to a modification in charge on the capsid surface and were present in 0.44 % and 5.11 %, respectively, of the ZIM/7/83 population. Antigenic profiling of ZIM/7/83 and vSAT2^{SNV} with three SAT2-specific scFvs (Opperman et al., 2012) indicated that the scFvs bound to the two viruses with the same binding profile (Table 3). Therefore, the four amino acid differences between ZIM/7/83 and vSAT2^{SNV} did not have a measurable effect on the antigenic structure of the virion.

Table 3
A summary of the variation observed in the outer capsid proteins between ZIM/7/83 and vSAT2^{SNV} and a comparison of the antigenicity as measured against three SAT2-specific single chain variable fragments (scFv).

Virus	Variation in amino acid sequence				Reactivity with SAT2-specific scFv*		
	1064	1093	1169	1212	scFv1	scFv2	scFv3
ZIM/7/83	G	G	H	K	1.2 ± 0.06	2.3 ± 0.08	2.4 ± 0.03
vSAT2^{SNV}	A	E	Y	E	1.4 ± 0.06	2.3 ± 0.01	2.3 ± 0.04

* The scFvs have been described in Opperman et al., 2012.

3.5. SAT2 viruses have a wide range of lability at low pH and high temperatures

The efficiency of viral progeny production depends on the efficiency of the capsid dissociation in the early endosome and the sensitivity of FMDV to acid is considered to be important for the release of the RNA genome into the cytoplasm (Curry et al., 1995; O'Donnell et al., 2005). To compare the stability of SAT2 virions during acidification the ZIM/7/83, vSAT2^{SNV}, ZIM/5/83, ZIM/14/90 and v^{EGY}SAT2 infectious viruses were incubated in pH buffers ranging from of 5.8–7.4 for 30 min, followed by titration on BHK-21 cells (Fig. 4A). The loss of SAT2 virus infectivity occurred over a relatively broad pH range with v^{EGY}SAT2 more resistant to low pH than the others. The ZIM/5/83 and ZIM/7/83 infectivity decreased by 53 % and 33 %, respectively, when incubated at pH 6.5 compared to physiological pH conditions (pH 7.4). ZIM/14/90 infectivity decreased by 58 %, from pH 7.4–6.5. The v^{EGY}SAT2 virus displayed the highest percentage of remaining infectious particles at pH 6.5 with a reduction of 13 % of the virus titre compared to that at pH 7.4. Although the vSAT2^{SNV} virus showed a somewhat faster decrease of infectious particles with decreasing pH compared to ZIM/7/83 it was not significant. The infectivity of the SAT2 virus particles decreased rapidly between pH 5.8 and 6.5. At the low pH range, the decline of infectious particles was not equal for the SAT2 viruses, with the infectivity of the ZIM/5/83, ZIM/7/83 and ZIM/14/90 viruses being reduced more rapidly below pH 6.3. At pH 5.8, even when the starting titres were normalized, the v^{EGY}SAT2 virus repeatedly resulted in *ca.* 900 infectious particles per ml, whilst no ZIM/14/90, ZIM/7/83 or vSAT2^{SNV} infectious particles were detectable below pH 6.0 (Fig. 4A). The pH_{50} can be described as the half-way point in

the transition of 146S infectious particles into 12S pentamers and can be used as a measure of pH sensitivity. The pH_{50} for ZIM/7/83 was calculated to be 6.62, whilst the pH_{50} of ZIM/5/83 and ZIM/14/90 was 6.68 and 6.66, respectively, whereas the pH_{50} of $vSAT2^{SNV}$ and $v^{EGY}SAT2$ was 6.77 and 6.47, respectively.

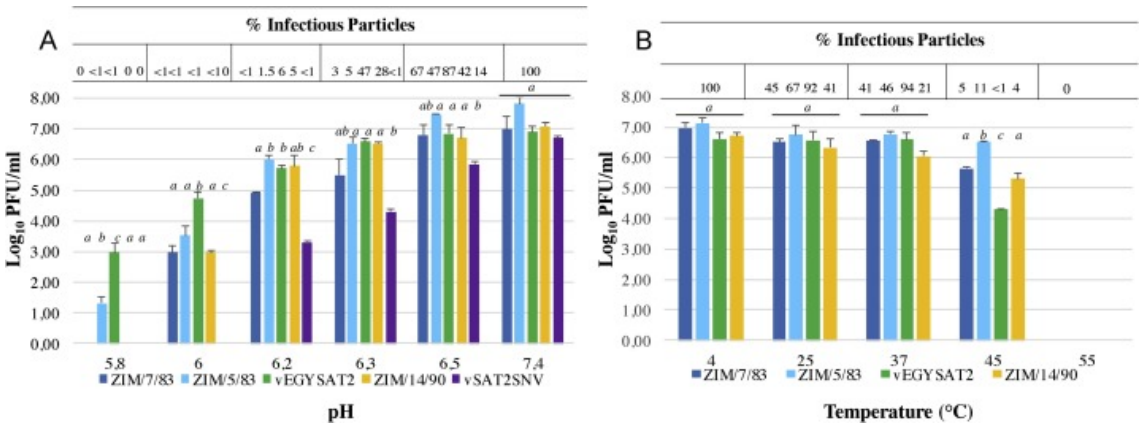

Fig. 4. (A) Evaluation of capsid stability of SAT2 viruses ZIM/5/83, ZIM/7/83, ZIM/14/90, $v^{EGY}SAT2$ and $vSAT2^{SNV}$ in different pH conditions. SDG-purified 146S virus particles were incubated in TNE (100 mM Tris, 150 mM NaCl, 10 mM EDTA) or MBS (25 mM MES, 150 mM NaCl, 10 mM EDTA) buffers ranging from pH 5.8 to 7.4 for 30 min, neutralised with 1 M Tris (pH 7.4) and titrated on BHK-21 cells. (B) The ZIM/5/83, ZIM/7/83, ZIM/14/90 and $v^{EGY}SAT2$ viruses were also incubated in physiological TNE at temperatures ranging from 4 °C to 55 °C and the remaining virus titre determined. The mean log_{10} virus titre of two inactivation experiments at each pH or temperature treatment was plotted and the error bars represent the standard deviation of the mean. The pH_{50} is defined as the pH value where the virus titre is halfway between the highest and lowest titre within the pH range 7.4 to 5.8 (Curry et al., 1995). The percentage of plaque forming units remaining after 30 min of incubation in different conditions is indicated at the top of the graph. The statistical groupings are depicted with lettering on the graph.

When incubated in a physiological buffer at temperatures ranging from 4 °C to 55 °C, the ZIM/5/83 and ZIM/7/83 viruses showed a similar decrease in titres with 42 %–46 % of infectious particles remaining after 30 min at 37 °C compared to titres at 4 °C, whilst ZIM/14/90 showed a 79 % decrease (Fig. 4B). However, incubation at 45 °C resulted in more than 95 % loss of ZIM/5/83, ZIM/7/83 and ZIM/14/90 infectivity and at 55 °C a complete loss of infectivity for all three SAT2 viruses was observed. Although more than 90 % of $v^{EGY}SAT2$ infectivity remained after 30-min treatment at 37 °C, infectivity decreased rapidly (to <1%) at 45 °C and no infectious particles could be detected at 55 °C.

4. Discussion

FMD SAT viruses have been reported to cause mild or subclinical infections that may be under-diagnosed in field conditions (Jori et al., 2009) and are likely to be more common than previously expected. The studies presented here demonstrate that not all SAT2 viruses are equally virulent in cattle. The two SAT2 viruses ZIM/5/83 and ZIM/7/83 were both highly attenuated in cattle, even after two rounds of passage in cattle, as observed by the mild clinical signs after needle challenge with ten-fold more virus compared to the highly virulent SAT2 strain ZIM/14/90. Both viruses evoked immune responses, although the detection of antibody titres using a liquid-phase blocking ELISA was delayed compared to ZIM/14/90-infected animals. No virus could be isolated from whole blood, but virus was present in a ZIM/14/90-infected animal's oropharynx during the acute phase of infection (data not shown). The mild FMD symptoms correlated with observations in the field where the

circulation of strains causing mild infections often go unnoticed in endemic regions (Jori et al., 2009). This has serious implications for the control of the disease. The attenuation of ZIM/5/83 and ZIM/7/83 viruses to cattle could not be directly linked to cell-culture adaptation, as previously reported for serotype O and C viruses (Sa-Carvalho et al., 1997; Baranowski et al., 1998; Bøtner et al., 2011). The ZIM/5/83 low passage virus and the ZIM/14/90 virus did not rapidly lyse BHK-21 cells and could not grow on CHO-K1 cells; therefore they lacked the ability to utilise HSPG for cell entry. However, after eight passages on BHK-21 cells, the ZIM/5/83 virus was able to infect CHO-K1 and CHO-lec2 cells, but the ZIM/14/90 virus was still unable to infect either cell line.

Data from real-time monitoring of growth in BHK-21 cell culture (Fig. S1) demonstrated that ZIM/7/83 more effectively killed BHK-21 cells *in situ* and grew to higher titres compared to the other SAT2 viruses, a feature linked to the number of passages in cell cultures. The *in situ* cell virulence did not reflect the pathogenesis of the viruses in cattle. ZIM/7/83 has been passaged multiple times in cell culture and is able to effectively lyse BHK-21 cells *in situ*, more so than its progenitor ZIM/5/83. It is known that viruses replicating in cell culture under constant environmental conditions result in the selection of progeny with an increased ability to lyse cells (Sevilla et al., 1996). Growth of the v^{EGY}SAT2 virus on cultured cells was somewhat delayed at 10–22 hpi, a feature that was also observed for ZIM/14/90 (Maree et al., 2013). The *in situ* growth properties of SAT2 viruses did not explain the pathogenesis in cattle.

The first essential step in the infection process of a virus *in vivo* or *in situ* is the recognition and binding to a cell surface receptor molecule. FMDV is known to use members of the integrin family to initiate infection, particularly the $\alpha_v\beta_6$ integrin receptor expressed on epithelium cells (Monaghan et al., 2005). However, it has been documented that variants of FMDV, virulent to cultured cells, emerge following serial cytolytic infections (Martinez et al., 1997; Sevilla et al., 1996). It is thought that FMDV adaptation to cell culture is made possible by the selective pressure of the viral quasispecies, exerted by the cell surface molecules that may act as virus receptors (Baranowski et al., 1998). Here we have shown that ZIM/7/83 acquired the ability to grow to high titres in BHK-21 cells, infect and replicate in CHO-K1, -677 and -745 cells, and lyse BHK-21 cells more rapidly than its progenitor, ZIM/5/83. The increased virulence in BHK-21 cells for ZIM/7/83 resulted in increased fitness. The viruses harbouring the ZIM/7/83 and EGY/09/12 capsids were subjected to a competition assay *in situ* and the ZIM/7/83 capsid successfully outcompeted EGY/09/12 and drove it to extinction even at a 10-fold higher initial titre for EGY/09/12. This is in agreement with findings of Mahapatra et al. (2015) who showed that cell culture-adapted virus acquires greater biological fitness in a co-infection competitive environment. However, both the vSAT2 and v^{EGY}SAT2 viruses were able to infect CHO-K1 cells. Replication of inter-serotype FMD viruses or variants derived from one original biological isolate (Martinez et al., 1991; Maree et al., 2016) have been assessed *in vitro* and in natural hosts. Experimental co-infection of SAT1, SAT2 and SAT3 viruses in buffalo or in cultured cells revealed that competition and fitness play a role in persistence (Maree et al., 2016). Fitness and virulence are unrelated virus traits (Herrera et al., 2007) and are dependent on the physical and biological environments in which the virus replication takes place (Domingo, 2010). Through repeated *in vitro* passage, the ZIM/07/83 capsid may have acquired high fitness, however, this does not imply pathogenesis in the *in vivo* environment (Maree et al., 2016).

This study shows that vSAT2 can initiate entry and replicate in CHO-677 and CHO-745 cells, which are rarely infected by FMDV. Previously, such observations of cell culture

tropism changes were demonstrated with a highly passaged FMD virus (Baranowski et al., 2000) or from selection in the presence of soluble $\alpha_v\beta_6$ integrin (Lawrence et al., 2013). Several studies have reported the presence of a third yet unidentified receptor additional to the defined HSPG and integrin receptors used by FMDV (Baranowski et al., 2000; Zhao et al., 2003; Berryman et al., 2013; Lawrence et al., 2013). It has been proposed that this integrin- and HSPG-independent entry of CHO cell lines is via the Jumonji C-domain containing protein 6 (JMJD6) (Lawrence et al., 2016).

The observed difference between viral fitness and virulence in the SAT2 viruses could be related to the observed amino acid differences in the capsid. The E1160 K substitution in the C-terminal end of the VP1 (1D) βG-βH loop and E1212 K in the C-terminus of VP1 (1D) represent a change in the amino acid character and both are surface exposed (Fig. 5). The two substitutions are the most likely determinants of the plaque phenotype on CHO-K1 cells and the point of interaction with the recombinant monoclonal antibodies scFv1 or scFv3 (Opperman et al., 2012).

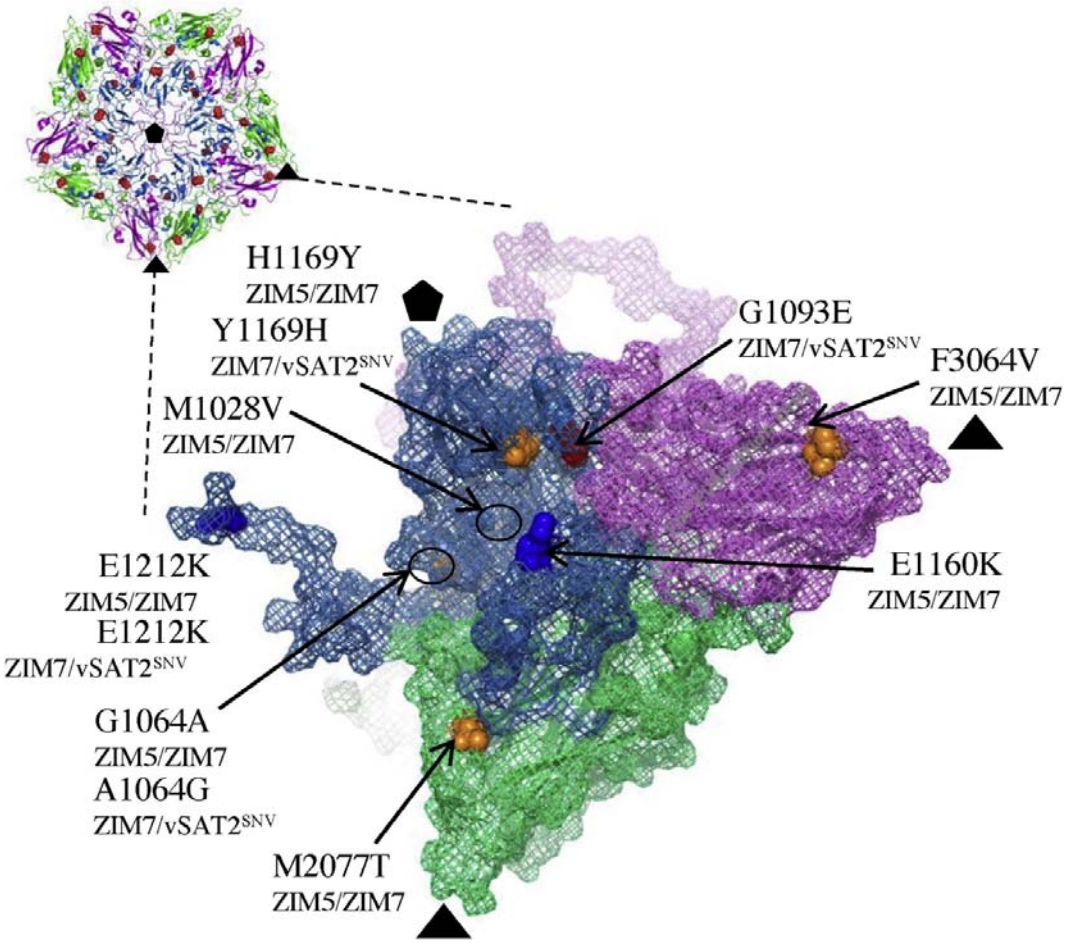

Fig. 5. Variation observed in VP1-3 capsid proteins in an amino acid alignment of ZIM/5/83, ZIM/7/83 and vSAT2^{SNV}, mapped to the structural models of the SAT2 (A) pentamers and (B) protomers. Variable positions are coloured in orange (no charge difference), blue (gain of positive charge) and red (gain of negative charge), VP1 (1D) in skyblue, VP2 (1B) in green and VP3 (1C) in magenta

Apart from genetic diversity between the two capsids, the effectiveness in release of viral RNA from the capsid depends on the stability of the capsid. Acid-induced dissociation of

FMDV particles within the endosome during replication results in the release of the genomic RNA, a feature that has been related to virulence *in situ* (Curry et al., 1995; Berryman et al., 2005; O'Donnell et al., 2005). Using SAT2 viruses, we demonstrated that the virus particles are relatively stable across a pH range of 6.6–7.4 with a pH_{50} of 6.5-6.6. Below pH 6.5 infectious SAT2 particles decrease rapidly; however, infectious particles of ZIM/5/83 and v^{EGY}SAT2 could be detected at pH 5.8. The acid lability of ZIM/7/83 observed here supports the findings of Scott et al. (2019) where the effect of pH on the shift of capsid dissociation temperatures was measured. It is hypothesised that the rapid early replication of ZIM/7/83 in cultured cells may partly be contributed by the rapid dissociation of the viral capsid by acidification in the early endosome. O'Donnell et al. (2005) showed that serotype O viral capsid protein was associated with early endosomes within 15 min following infection of cultured cells, but undetectable by 30 min after infection. The thermostability of the SAT2 capsids were comparable across the temperature range of 4−45 °C, whereas no infectious SAT2 particles were observed after 30-min treatment at 55 °C in a physiological buffer. Although our data suggest a link between cell virulence and acid lability of the SAT2 viral capsid, no direct correlation could be found between virus capsid lability and pathogenesis in cattle.

The biophysical stability characterization of the recombinant mutant $vSAT2^{SNV}$ virus, originating from the ZIM/7/83 virus quasispecies population, revealed that it was more sensitive than vSAT2 when exposed to mild acidic pH treatment. The $vSAT2^{SNV}$ virus was also unable to infect and replicate in CHO-K1 cells, did not replicate to high titres in BHK-21 cells, but antigenically could not be distinguished from vSAT2. The amino acid substitutions in the capsid proteins of $vSAT2^{SNV}$ were all found in the original ZIM/7/83 virus population, albeit at different levels of representation.

The results reported here emphasize the genetic flexibility and adaptive potential of RNA viruses' quasispecies genomes. Indeed, these enable RNA viruses to adapt rapidly to changing environments to advance in fitness or virulence *in situ* or *in vivo*. The variance in pathogenesis of SAT2 viruses did not correlate with virulence in cultured cells or viral fitness during co-infection of cultured cells. The biophysical stability of SAT2 viruses investigated revealed that SAT2 viruses have a wide range of lability at low pH or high temperatures with no direct correlation with pathogenesis. This has implications for the emergence of new viruses in nature and therefore the effective control of SAT2 viruses needs to consider the variance in biological phenotypes attributed to survival and increased spread.

Acknowledgements

Research findings documented in this manuscript were in part supported by funding from MSD Animal Health (previously Intervet SPAH) and a cooperative research and development agreement between the Agricultural Research Council, Onderstepoort Veterinary Institute (ARC-OVI) of South Africa and the United States Department of Agriculture, Agricultural Research Service, agreement number 58-3K95-M-894. Additional financial support was received from the Vaccine Initiative (ESCP). The authors would like to express their sincere gratitude to Dr D. Goovaerts and Dr E. Rieder for many fruitful discussions. The authors would like to express their gratitude to the personnel at Transboundary Animal Diseases (TAD) of the ARC-OVI for their contributions to virus isolation and animal work. Many thanks to Mr Jan Esterhuysen for his contribution with performing VNTs. We would also like to thank Drs A. Pretorius, D. Wallace and M. van Kleef for commenting and critical reading of the manuscript.

References

Acharya, R., Fry, E., Stuart, D., Fox, G., Rowlands, D., Brown, F., 1989. The three-dimensional structure of foot-and-mouth disease virus at 2.9 Å resolution. *Nature* 337, 709–716.

Ahmed, H.A., Salem, S.A.H., Habashi, A.R., Arafa, A.A., Aggour, M.G.A., Salem, G.H., Gaber, A.S., Selem, O., Abdelkader, S.H., Knowles, N.J., Madi, M., Valdazo-Gonzalez, B., Wadsworth, J., Hutchings, G.H., Mioulet, V., Hammond, J.M., King, D.P., 2012. Emergence of foot-and-Mouth disease virus SAT 2 in Egypt during 2012. *Transbound.Emerg. Dis*. 59, 476–481.

Baranowski, E., Sevilla, N., Verdaguer, N., Ruiz-Jarabo, C.M., Beck, E., Domingo, E., 1998. Multiple virulence determinants of foot-and-mouth disease virus in cell culture. *J. Virol.* 72, 6362–6372.

Baranowski, E., Ruiz-Jarabo, C.M., Sevilla, N., Andreu, D., Beck, E., Domingo, E., 2000. Cell recognition by foot-and-mouth disease virus that lacks the RGD integrin-binding motif: flexibility in aphthovirus receptor usage. *J. Virol*. 74, 1641–1647.

Berinstein, A., Roivainen, M., Hovi, T., Mason, P.W., Baxt, B., 1995. Antibodies to the vitronectin receptor (integrin αVβ3) inhibit binding and infection of foot-and-mouth disease virus to cultured cells. *J. Virol*. 69 (4), 2664–2666.

Berryman, S., Clark, S., Monaghan, P., Jackson, T., 2005. Early events in integrin alphavbeta6-mediated cell entry of foot-and-mouth disease virus. *J. Virol*. 79, 8519–8534.

Berryman, S., Clark, S., Kakker, N.K., Silk, R., Seago, J., Wadsworth, J., Chamberlain, K., Knowles, N.J., Jackson, T., 2013. Positively charged residues at the five-fold symmetry Axis of cell culture-adapted foot-and-Mouth disease virus permit novel receptor interactions. *J. Virol*. 87 (15), 8735–8744.

Bøtner, A., Kakker, N.K., Barbezange, C., Berryman, S., Jackson, T., Belsham, G.J., 2011. Capsid proteins from field strains of foot-and-mouth disease virus confer a pathogenic phenotype in cattle on an attenuated, cell-culture-adapted virus. *J. Gen. Virol.* 92, 1141–1151.

Brehm, K.E., Ferris, N.P., Lenk, M., Riebe, R., Haas, B., 2009. Highly sensitive fetal goat tongue cell line for detection and isolation of foot-and-mouth disease virus. *J. Clin Microbiol*. 47, 3156–3160.

Bronsvoort, B.M., Radford, A.D., Tanya, V.N., Nfon, C., Kitching, R.P., Morgan, K.L., 2004. Molecular epidemiology of foot-and-mouth disease viruses in the Adamawa province of Cameroon. *J. Clin. Microbiol*. 42, 2186–2196.

Callahan, J.D., Brown, F., Osorio, F.A., Sur, J.H., Kramer, E., Long, G.W., Lubroth, J., Ellis, S.J., Shoulars, K.S., Gaffney, K.L., Rock, D.L., Nelson, W.M., 2002. Use of a portable real-time reverse transcriptase-polymerase chain reaction assay for rapid detection of foot-and-mouth disease virus. *J. Am. Vet. Med. Ass.* 220, 1636–1642.

Casey-Bryars, M., Reeve, R., Bastola, U., Knowles, N.J., Auty, H., Bachanek-Bankowska, K., et al., 2018. Waves of endemic foot-and-mouth disease in eastern Africa suggest feasibility of proactive vaccination approaches. *Nat. Ecol. Evol.* 2 (9), 1449–1457.

Curry, S., Abrams, C.C., Fry, E., Crowther, J.C., Belsham, G.J., Stuart, D.I., King, A.M.Q., 1995. Viral RNA modulates the acid sensitivity of Foot-and-mouth disease virus capsids. *Amer. Soc. Micro.* 69, 430–438.

Curry, S., Fry, E., Blakemore, W., Abu-Ghazaleh, R., Jackson, T., 1997. Dissecting the roles of VP0 cleavage and RNA packaging in picornavirus capsid stabilization: the structure of empty capsids of foot-and-mouth disease virus. J. Virol. 71, 9743–9752.

Dawe, P.S., Flanagan, F.O., Madekurozwa, R.L., Sorensen, K.J., Anderson, E.C., Foggin, C.M., Ferris, N.P., Knowles, N.J., 1994. Natural transmission of foot-and-mouth disease virus from African buffalo (*Syncerus caffer*) to cattle in a wildlife area of Zimbabwe. *Vet. Rec*. 134, 230–232.

Doel, T.R., Mowat, G.N., 1985. An international collaborative study on foot and mouth disease virus assay methods. 2. Quantification of 146S particles. *J. Biol. Stand*. 13, 335–344.

Domingo, E., 2010. Mechanisms of viral emergence. *Vet. Res.* 41 (6), 38.

Ellard, F.M., Drew, J., Blakemore, W.E., Stuart, D.I., King, A.M.Q., 1999. Evidence for the role of His-142 of protein lC in the acid-induced disassembly of foot-and-mouth disease virus capsids. *J. Gen. Virol*. 80, 1911–1918.

Feigelstock, D., Mateu, M.G., Piccone, M.E., de Simone, F., Brocchi, E., Domingo, E., Palma, E.L., 1992. Extensive antigenic diversification of foot-and-mouth disease virus by amino acid substitutions outside the major antigenic site. *J. Gen. Virol*. 73, 3307–3311.

Fry, E.E., Newman, J.W.I., Curry, S., Najjam, S., Jackson, T., Blakemore, W., Lea, S.M., Miller, L., Burman, A., King, A.M.Q., Stuart, D.I., 2005. Structure of FMDV serotype A1O61 alone and complexed with oligosaccharide receptor: receptor conservation in the face of antigenic variation. *J. Gen. Virol*. 86, 1909–1920.

Jackson, T., Ellard, F.M., Ghazaleh, R.A., Brookes, S.M., Blakemore, W.E., Corteyn, A.H., Stuart, D.I., Newman, J.W.I., King, A.M.Q., 1996. Efficient infection of cells in culture by type O foot-and-mouth disease virus requires binding to cell surface heparin sulfate. *J. Virol*. 70, 5282–5287.

Jackson, T., Sheppard, D., Denyer, M.N., Blakemore, W., King, A.M.Q., 2000. The epithelial integrin αvβ6 is a receptor for foot-and-Mouth disease virus. *J. Virol*. 74 (11), 4949–4956.

Jackson, T., Mould, A.P., Sheppard, D., King, A.M.Q., 2002. Integrin αvβ1 is a receptor for Foot-and-mouth disease virus. *J. Virol.* 76 (3), 935–941.

Jori, F., Vosloo, W., Du Plessis, B., Bengis, R., Brahmbhatt, D., Gummow, B., Thomson, G.R., 2009. A qualitative risk assessment of factors contributing to foot and mouth disease outbreaks in cattle along the western boundary of the Kruger National Park. *Rev. Sci. Tech.* 28 (3), 917–931.

Knight-Jones, T.J., Rushton, J., 2013. The economic impacts of foot and mouth disease – what are they, how big are they and where do they occur? *Prev. Vet. Med.* 112 (3–4), 161–173.

Knipe, T., Rieder, E., Baxt, B., Ward, G., Mason, P.W., 1997. Characterization of synthetic foot-and-mouth disease virus provirions separates acid-mediated disassembly from infectivity. *J. Virol*. 71, 2851–2856.

Kotecha, A., Seago, J., Scott, K., Burman, A., Loureiro, S., Ren, J., et al., 2015. Structure-based energetics of protein interfaces guides foot-and-mouth disease virus vaccine design. *Nat. Struc. and Mol. Boil*. 22, 788–794.

Lawrence, P., LaRocco, M., Baxt, B., Rieder, E., 2013. Examination of soluble integrin resistant mutants of foot-and-mouth disease virus. *Virol. J.* 10, 2.

Lawrence, P., Pacheco, J., Stenfeldt, C., Arzt, J., Rai, D.K., Rieder, E., 2016. Pathogenesis and micro-anatomic characterization of a cell-adapted mutant foot-and-mouth disease virus in cattle: impact of the Jumonji C-domain containing protein 6 (JMJD6) and route of inoculation. *Virology* 492, 108–117.

Logan, D., Abu-Ghazaleh, D., Blakemore, W., Curry, S., Jackson, T., King, A., Lea, S., Lewis, R., Newman, J., Parry, N., Rowlands, D., Stuart, D., Fry, E., 1993. Structure of a major immunogenic site on foot-and-mouth disease virus. *Nature* 362, 566–568.

Mahapatra, M., Yuvaraj, S., Madhanmohan, M., Subramaniam, S., Pattnaik, B., Paton, D.J., Srinivasan, V.A., Parida, S., 2015. Antigenic and genetic comparison of foot-and-mouth disease virus serotype O Indian vaccine strain, O/IND/R2/75 against currently circulating viruses. *Vaccine* 33 (5), 693–700.

Maree, F.F., Blignaut, B., Esterhuysen, J.J., De Beer, T.A.P., Theron, J., O'Neil, H.G., Rieder, E., 2011. Predicting antigenic sites on the foot-and-mouth disease virus capsid of the South African Territories (SAT) types using virus neutralization data. *J. Gen. Virol*. 92, 2297–2309.

Maree, F.F., Blignaut, B., de Beer, T.A., Rieder, E., 2013. Analysis of SAT type foot-and-mouth disease virus capsid proteins and the identification of putative amino acid residues affecting virus stability. *PLoS One* 8 (5), e61612.

Maree, F.F., de Klerk-Lorist, L.-M., Gubbins, S., Zhang, F., Seago, J., Pérez-Martín, E., Reid, E., Scott, K.A., van Schalkwyk, L., Bengis, R., Charleston, B., Juleff, N., 2016. Differential persistence of foot-and-mouth disease virus in African buffalo is related to virus virulence. *J. Virol.* 90 (10), 5132–5140.

Martinez, M.A., Carrillo, C., Gonzalez-Candelas, F., Moya, A., Domingo, E., Sobrino, F., 1991. Fitness alteration of foot-and-mouth disease virus mutants: measurement of adaptability of viral quasispecies. *J. Virol*. 65, 3954–3957.

Martinez, M.A., Verdaguer, N., Mateu, M.G., Domingo, E., 1997. Evolution subverting essentiality: dispensability of the cell attachment Arg-Gly-Asp motif in multiply passaged foot-and-mouth disease virus. Proc. Nat. Acad. Sci. 94, 6798–6802.

Monaghan, P., Gold, S., Simpson, J., Zhang, Z., Weinreb, P.H., Violette, S.M., Alexandersen, S., Jackson, T., 2005. The avb6 integrin receptor for Foot-and-mouth disease virus is expressed constitutively on the epithelial cells targeted in cattle. *J. Gen. Virol*. 86, 2769–2780.

Neff, S., Mason, P.W., Baxt, B., 2000. High-efficiency utilization of the bovine integrin αVβ3 as a receptor for foot-and-mouth disease virus is dependent on the bovine β3 subunit. *J. Virol.* 74, 7298–7306.
O'Donnell, V., La Rocco, M., Duque, H., Baxt, B., 2005. Analysis of Foot-and-mouth disease virus internalization events in cultured cells. *J. Virol*. 79, 8506–8518.

OIE, 2018. *Manual of Diagnostic Tests and Vaccines for Terrestrial Animals*. Office International des Epizooties, Paris.

Opperman, P.A., Maree, F.F., Van Wyngaardt, W., Vosloo, W., Theron, J., 2012. Mapping of antigenic determinants on a SAT2 foot-and-mouth disease virus using chicken single-chain antibody fragments. *Virus Res*. 167 (2), 370–379.

Opperman, P.A., Rotherham, L.S., Esterhuyzen, J., Charleston, B., Juleff, N., Capozzo, A.V., Theron, J., Maree, F.F., 2014. Determining the Epitope Dominance on the Capsid of a serotype SAT2 Foot-and-mouth disease virus by mutational analyses. *J. Virol.* 88, 8307–8318.

Pacheco, J.M., Henry, T.M., O'Donnell, V.K., Gregory, J.B., Mason, P.W., 2003. Role of nonstructural proteins 3A and 3B in host range and pathogenicity of foot-and-mouth disease virus. *J. Virol. 77*, 13017–13027.

Pacheco, J.M., Piccone, M.E., Rieder, E., Pauszek, S.J., Borca, M.V., Rodriguez, L.L., 2010. Domain disruptions of individual 3B proteins of foot-and-mouth disease virus do not alter growth in cell culture or virulence in cattle. *Virology* 405 (1), 149–156.

Reeve, R., Blignaut, B., Esterhuysen, J.J., Opperman, P., Matthews, L., Fry, E.E., de Beer, T.A., Theron, J., Rieder, E., et al., 2010. Sequence-based prediction for vaccine strain selection and identification of antigenic variability in foot-and-mouth disease virus. *PLoS Comput. Biol*. 6, e1001027.

Rieder, E., Bunch, T., Brown, F., Mason, P.W., 1993. Genetically engineered foot-and-mouth disease viruses with poly(C) tracts of two nucleotides are virulent in mice. *J. Virol*. 67, 5139–5145.

Rweyemamu, M., Roeder, P., Mackay, D., et al., 2008. Epidemiological patterns of foot-and-mouth disease worldwide. *Transbound. Emerg. Dis*. 55, 57–72.

Sa-Carvalho, D., Rieder, E., Baxt, B., Rodarte, R., Tanuri, A., Mason, P.W., 1997. Tissue culture adaptation of foot-and-mouth disease virus selects viruses that bind to heparin and are attenuated in cattle. *J. Virol*. 71, 5115–5123.

Sevilla, N., Vedaguer, N., Domingo, E., 1996. Antigenically profound amino acid substitutions occur during large population passages of foot-and-mouth disease virus. *Virology* 225, 400–405.

Thompson, J.D., Gibson, T.J., Plewniak, F., Jeanmougin, F., Higgins, D.G., 1997. The CLUSTAL_X windows interface: flexible strategies for multiple sequence alignment aided by quality analysis tools. *Nucleic Acids Res.* 25, 4876–4882.

Thomson, G.R., Vosloo, W., Bastos, A.D.S., 2003. Foot and mouth disease in wildlife. *Virus Res*. 91, 145–161.

Valdazo-González, B., Knowles, N.J., Hammond, J., King, D.P., 2012. Genome sequences of SAT 2 foot-and-Mouth disease viruses from Egypt and Palestinian autonomous territories (Gaza Strip). *J. Virol*. 86, 8901–8902.

Van Rensburg, H.G., Henry, T., Mason, P.W., 2004. Studies of genetically defined chimeras of a European type A virus and a South African Territories type 2 virus reveal growth determinants for foot-and-mouth disease virus. *J. Gen. Virol*. 85, 61–68.

Vosloo, W., Bastos, A.D.S., Sangare, O., Hargreaves, S.K., Thomson, G.R., 2002. Review of the status and control of foot and mouth disease in sub-Saharan Africa. *Rev. Sci. Tech. OIE*. 21, 437–449.

Zaher, K.S., Syame, S.M., Elhewairy, H.M., Marie, S.H.M., 2014. Investigation of foot-and-mouth disease outbreak in Egyptian buffalo-cows in 2012. *Glob. Vet*. 12 (5), 660–666.

Zhao, Q., Pacheco, J.M., Mason, P.W., 2003. Evaluation of genetically engineered derivatives of a Chinese strain of foot-and-mouth disease virus reveals a novel cell-binding site which functions in cell culture and in animals. *J. Virol*. 77, 3269–3280.